SAMSUNG

Ultrasound and MV-CEUS™ (Microvascular Contrast-Enhanced Ultrasound) in Liver Diagnostics

Dirk-André Clevert, MD, PhD
Interdisciplinary Ultrasound Center at the Munich University Hospital – Grosshadern (Germany)

Introduction

Ultrasound has evolved into one of the most frequently employed imaging modalities in hepatology. It is usually the first diagnostic tool applied when patients present with elevated liver enzymes, suspected fatty liver disease, cirrhosis, or space-occupying lesions. This preference is due to a combination of safety, accessibility, and cost-effectiveness. Unlike CT and MRI, ultrasound is widely available, portable, and does not require ionizing radiation.

In clinical routine, conventional B-mode ultrasound provides basic information about liver size, echotexture, and the presence of focal abnormalities. It is indispensable in screening for diffuse parenchymal diseases such as steatosis and fibrosis. The diagnostic spectrum is greatly expanded by Doppler and power Doppler imaging, which assess macrovascular blood flow in the hepatic artery, portal vein, and hepatic veins. These techniques are valuable in conditions such as portal hypertension, Budd–Chiari syndrome, or after liver transplantation.

Regular follow-up imaging is crucial for patients with chronic liver conditions to detect changes early and adjust treatment plans accordingly [1]. Ultrasound does not use ionizing radiation, making it safe for repeated use, including in pregnant women and children [2-6]. It provides dynamic assessment and immediate results, which is essential for guiding interventional procedures. Compared to other imaging modalities like CT and MRI, ultrasound is less expensive and widely available, making it a practical choice for many healthcare settings [7].

The advent of contrast-enhanced ultrasound (CEUS) has further strengthened the role of ultrasound in liver imaging. CEUS enables dynamic assessment of vascularity and perfusion patterns in focal liver lesions in real time. In many cases, it allows a reliable differentiation between benign lesions such as hemangiomas or focal nodular hyperplasia and malignant lesions such as hepatocellular carcinoma (HCC) or metastases [8]. The ability to avoid unnecessary biopsy or surgery is of significant clinical relevance.

However, reliable differentiation between benign and malignant findings can remain challenging in individual patients. Conventional grayscale imaging and CEUS, while powerful, may not always provide the necessary resolution to visualize fine vascular details that could guide precise diagnosis. For this reason, new technologies such as Super Resolution (SR) Imaging have emerged to overcome these limitations [9-12].

Materials and Methods

Technical background

Super Resolution (SR) Imaging in ultrasound enhances microvascular visualization by localizing individual contrast microbubbles over time, enabling the reconstruction of structures at a higher resolution than conventional CEUS. Each bubble is localized with subwavelength precision, and thousands of positions are combined to reconstruct a vascular map far beyond the diffraction limit of conventional ultrasound [13-15].

This approach allows for the visualization of vessels at the capillary scale, which were previously invisible. By enabling 4–8 times higher resolution than standard CEUS, SR imaging provides a detailed map of the microvascular architecture [16-17]. The clinical implications are substantial: tumor angiogenesis, treatment response, and microcirculatory changes can be studied in a way that was previously reserved for histology or experimental techniques.

Two key SR-derived parameters have gained particular relevance:

- **Microvascular CEUS**: provides an enhancement of perfused microvasculature within a lesion or region of interest. Rich vascularization can indicate malignancy or hypervascular benign lesions, while sparse microcirculation may suggest necrosis or fibrosis.
- **Time of Arrival (TOA)**: analyzes the temporal sequence of contrast filling within a lesion. It provides information on how rapidly microbubbles reach specific regions and how enhancement evolves over time. TOA has proven valuable for differentiating fast-arterialized malignancies from slowly enhancing benign lesions.

In addition to these, other experimental SR parameters are under evaluation, including vessel tortuosity indices and heterogeneity scores, which may refine the understanding of tumor biology.

From a technical perspective, motion artifacts remain a challenge, particularly in abdominal imaging where breathing and peristalsis introduce variability. Solutions include motion compensation algorithms and ultrafast frame rates, which improve stability and reproducibility. In routine practice, modern ultrasound machines already incorporate motion correction modes to facilitate SR imaging.

MV-CEUS™ (Microvascular Contrast-Enhanced Ultrasound)

MV-CEUS™ is the Super Resolution Imaging feature of Samsung's new premium ultrasound system (R20), providing advanced image processing for CEUS images to enable enhanced visualization of microvascular structures. Powered by proprietary non-rigid elastic motion estimation, it aims to address key challenges of conventional ULM (Ultrasound Localization Microscopy) methods, including motion artifacts, dependency on microbubble dosage, and long processing times.

MV-CEUS™ can operate in a live mode, allowing users to activate it in real time during a standard CEUS scan. This eliminates the need to switch modes or wait of offline processing, a capability that is critical for the dynamic assessment of pathology. During the arterial phase, MV-CEUS™ provides enhanced view of vascular structure, allowing clinicians to observe rapid inflow patterns. Furthermore, the Time of Arrival (TOA) map provides an immediate and intuitive visualization of contrast wash-in time across the entire image.

Clinical Applications

Benign Lesions

While most hemangiomas, focal nodular hyperplasia or hepatocellular adenoma can be characterized with CEUS, atypical cases remain problematic. The clinical results below demonstrate that MV-CEUS™ is more discriminative than conventional Doppler, as it allows for the analysis of microvascular homogeneity and arterial filling patterns, suggesting that it could reduce unnecessary MRI or biopsy.

Case 1) Hemangiomas (Fig. 1-6)

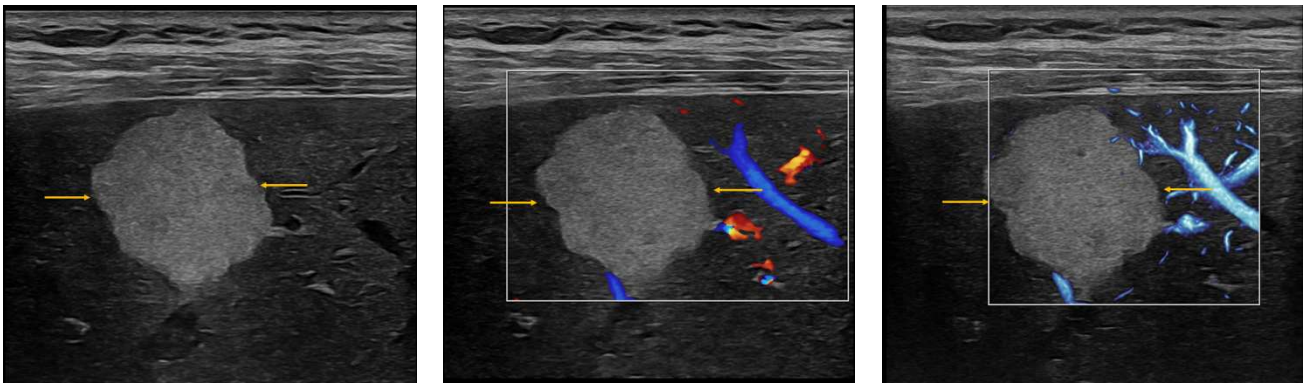

Figure 1: 40-year-old female patient with hyperechoic lesion (yellow arrows, diameter is about 10mm) in a non-cirrhotic liver. A linear probe was used for the high-resolution examination

Figure 2: The hyperechoic lesion (yellow arrows) does not display an increase vascularization in **color** duplex sonography.

Figure 3: The hyperechoic lesion (yellow arrows) does not display an increase central vascularization, only the peripheral some tiny vessels are detected by **MV-Flow™**.

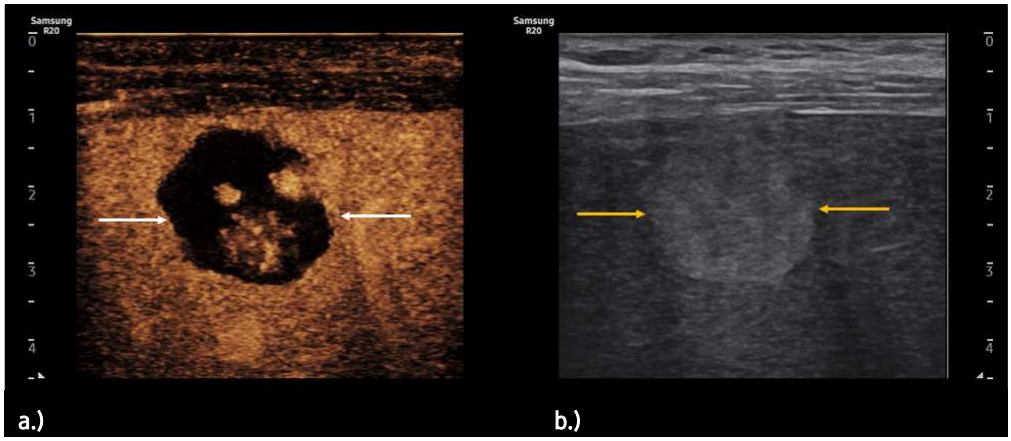

Figure 4: Dual-mode technique showing **CEUS** information (a.) and the B-scan (b.). In the **arterial phase**, the lesion is delineated by peripheral nodular enhancement (white arrows) in the contrast image and additional seen in the B-scan (yellow arrows).

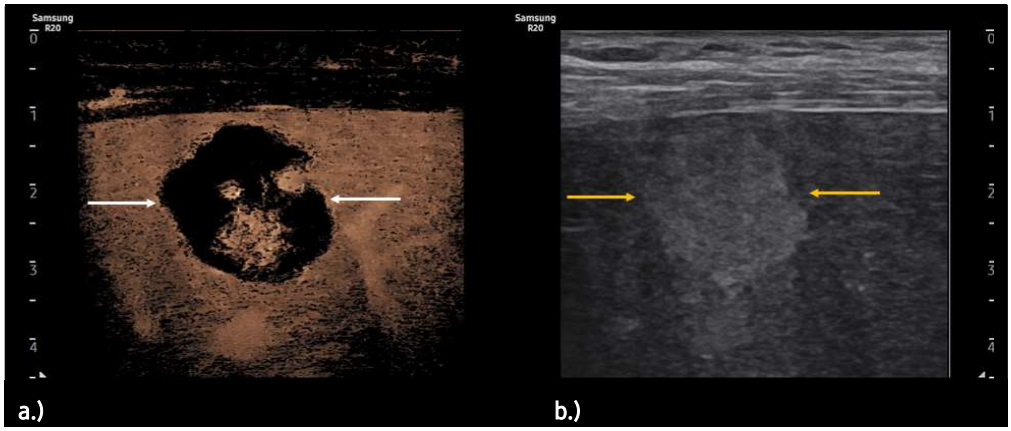

Figure 5: Dual-mode technique showing **MV-CEUS™** (a.) and the B-scan (b.). In the **arterial phase**, the lesion is delineated by peripheral nodular enhancement (white arrows) in the **MV-CEUS™**. The lesion is additional seen in the B-scan (yellow arrows). The final diagnosis was a partial thrombotic hemangioma.

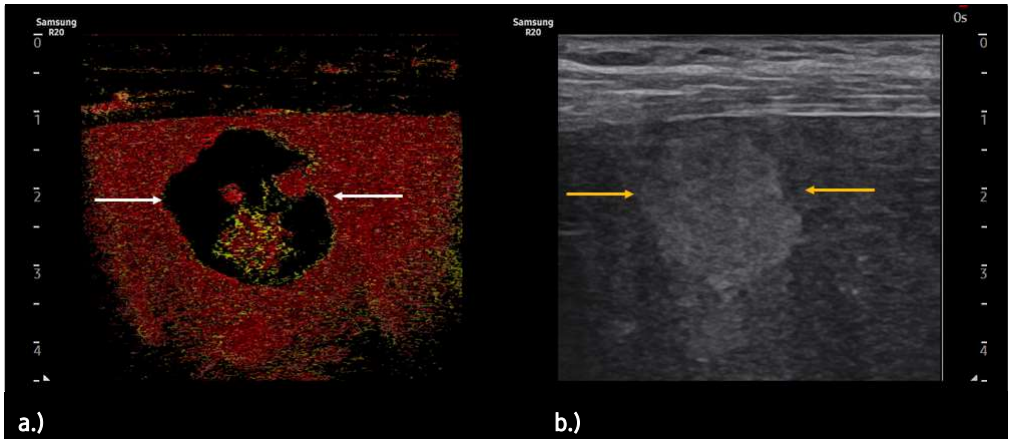

Figure 6: Dual-mode technique showing **Time of arrival** (a.) and the B-scan (b.). In the **arterial phase**, the lesion is delineated by peripheral nodular enhancement (white arrows) in comparison to the surrounding tissue the perinodular enhancement has got a delay in enhancement in the **Time of arrival**. The lesion is additional seen in the B-scan (yellow arrows). The final diagnosis was a partial thrombotic hemangioma.

Case 2) Focal Nodular Hyperplasia (Fig. 7-12)

Figure 7: 23-year-old female patient with an isoechoic lesion (yellow arrows). The diameter of the lesion is round about 8 cm.

Figure 8: The liver lesion (yellow arrows) displays an increased vascularization in **color** duplex sonography

Figure 9: The liver lesion (yellow arrows) displays an increased vascularization in **MV-Flow™**.

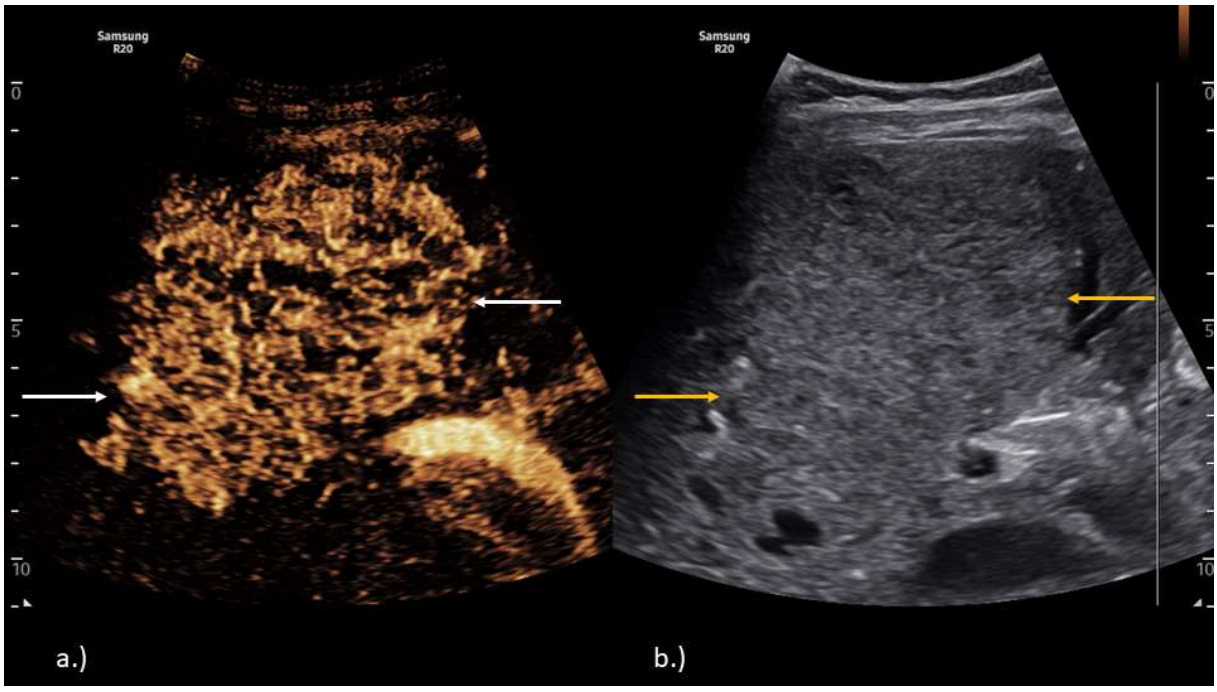

Figure 10: Dual-mode technique showing **CEUS** information (a.) and the B-scan (b.). In the **arterial phase**, the lesion is delineated by a strong hyperenhancement (white arrows) in the contrast image and additional seen in the B-scan (yellow arrows).

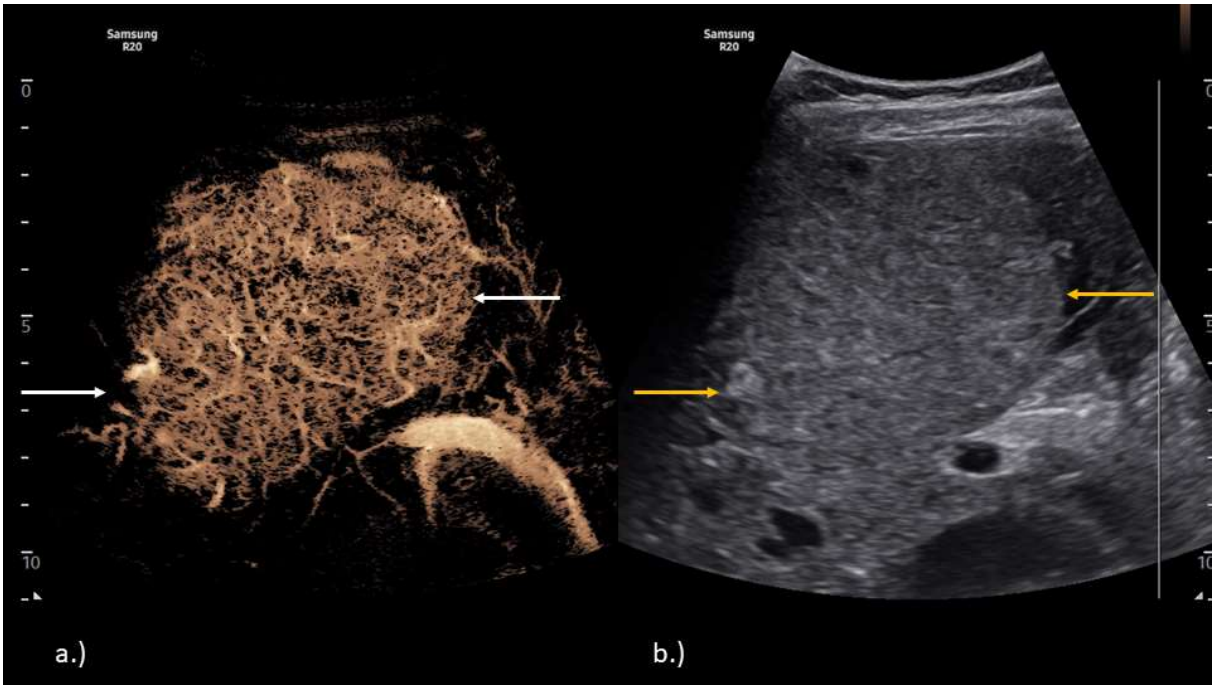

Figure 11: Dual-mode technique showing **MV-CEUS™** (a.) and the B-scan (b.). In the **arterial phase**, the lesion is delineated by a strong hyperenhancement (white arrows) in the **MV-CEUS™**, tiny vessels are visible. The lesion is additional seen in the B-scan (yellow arrows). The final diagnosis was a huge Focal nodular hyperplasia (FNH).

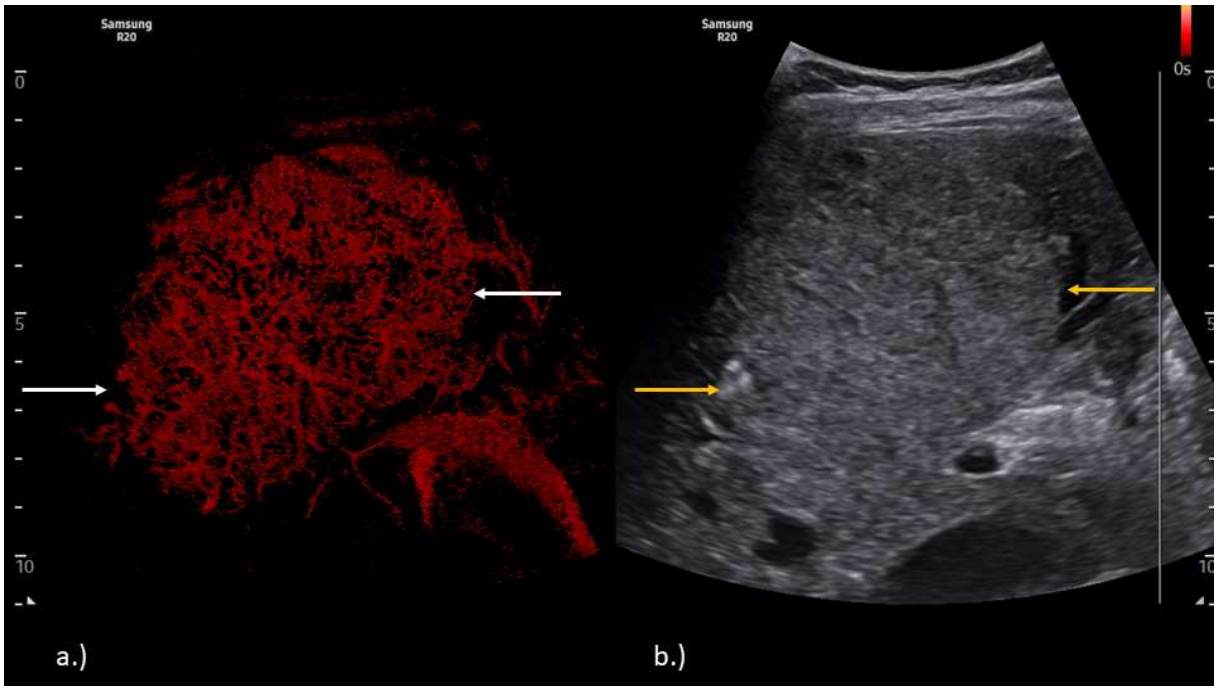

Figure 12: Dual-mode technique showing **Time of arrival** (a.) and the B-scan (b.). In the **arterial phase**, the lesion is delineated by a strong and fast hyperenhancement (white arrows) in the **Time of arrival**. The lesion is additional seen in the B-scan (yellow arrows). The final diagnosis was a huge Focal nodular hyperplasia (FNH).

Case 3) Hepatocellular Adenoma (Fig. 13-18)

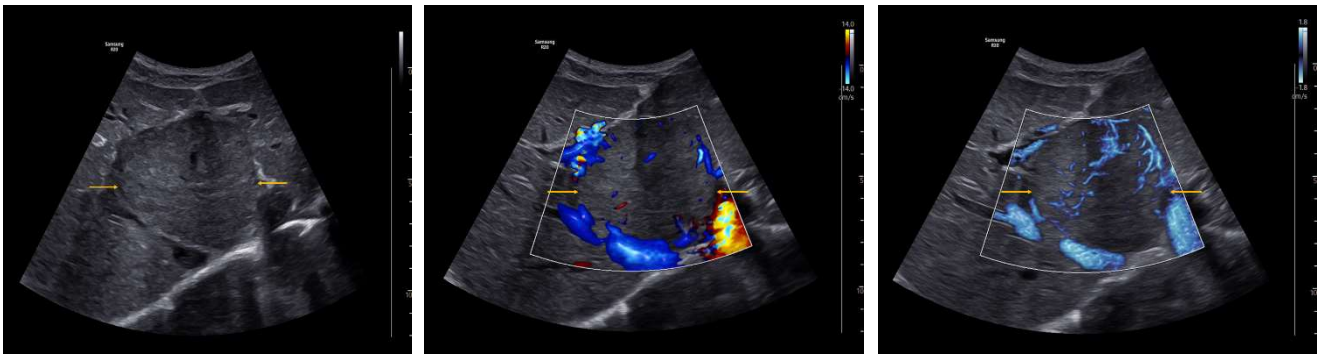

Figure 13: 33-year-old female patient with an isoechoic lesion (yellow arrows). The diameter of the lesion is round about 8 cm.

Figure 14: The liver lesion (yellow arrows) displays an increased peripheral vascularization in **color** duplex sonography.

Figure 15: The liver lesion (yellow arrows) displays an increased peripheral and central vascularization in **MV-Flow™**.

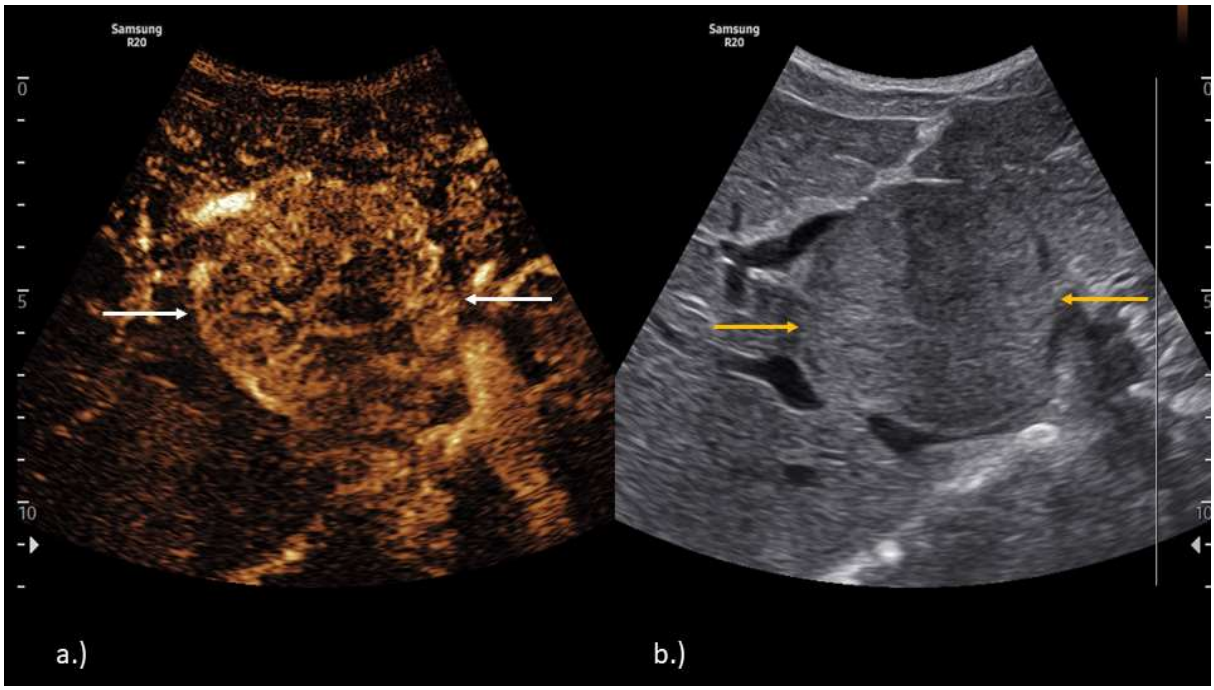

Figure 16: Dual-mode technique showing **CEUS** information (a.) and the B-scan (b.). In the **arterial phase**, the lesion is delineated by a strong enhancement from the peripheral to the center (white arrows) in the contrast image and additional seen in the B-scan (yellow arrows).

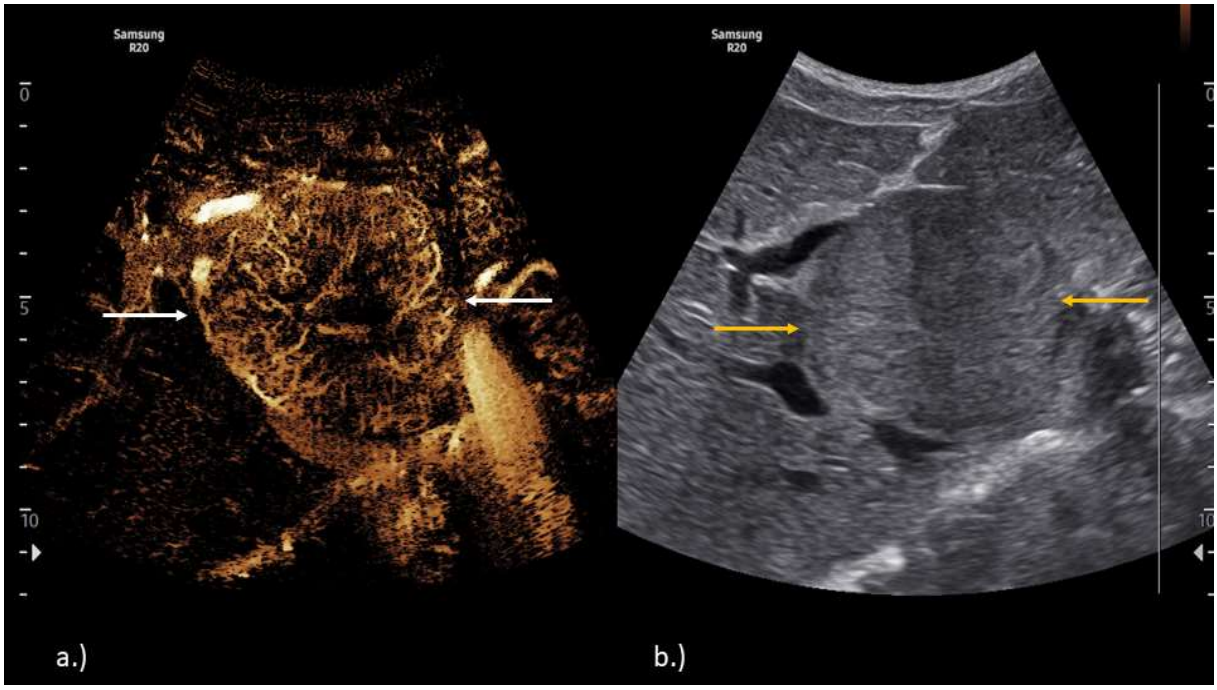

Figure 17: Dual-mode technique showing **MV-CEUS™** (a.) and the B-scan (b.). In the **arterial phase**, the lesion is delineated by a strong enhancement from the peripheral to the center (white arrows) in **MV-CEUS™**, tiny feeding vessel are visible. The lesion is additional seen in the B-scan (yellow arrows). The final diagnosis was a huge hepatocellular adenoma.

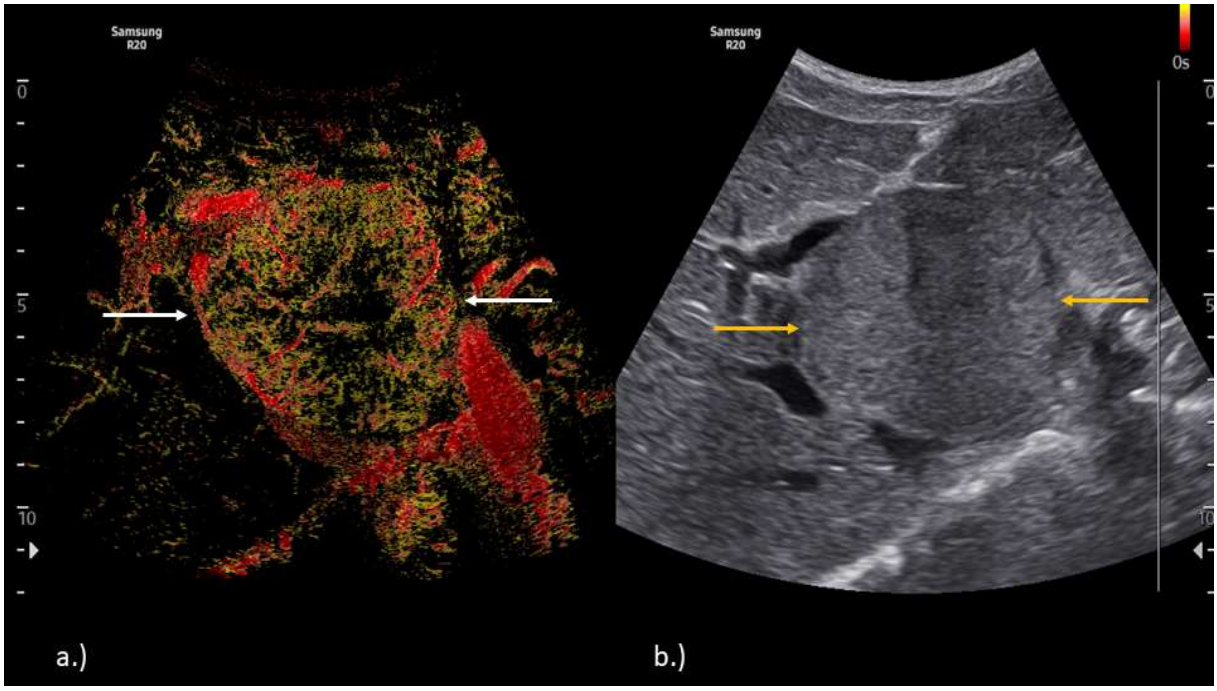

Figure 18: Dual-mode technique showing **Time of arrival** (a.) and the B-scan (b.). In the **arterial phase**, the lesion is delineated by a strong enhancement from the peripheral to the center (white arrows) in the **Time of arrival**. Tiny feeding vessels are visible. The lesion is additional seen in the B-scan (yellow arrows). The final diagnosis was a huge hepatocellular adenoma.

Metastases and Lymphoma (Fig. 19-24)

In patients with colorectal or breast cancer, early detection of liver metastases is critical for curative strategies. Small metastases may remain inconspicuous in grayscale ultrasound but can demonstrate distinct perfusion deficits on CEUS. MV-CEUS™ adds another dimension by revealing disrupted microvascular architecture and highlighting micrometastatic vascular patterns.

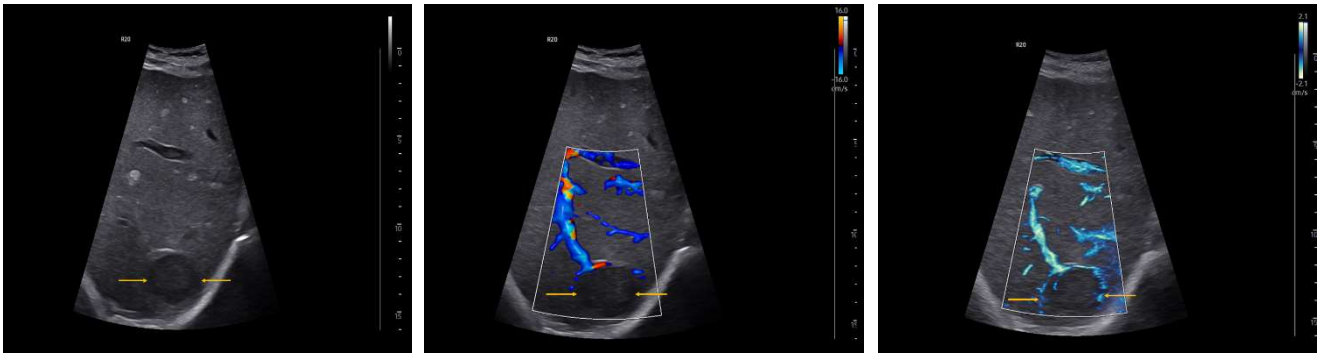

Figure 19: 38-year-old female patient with a hypoechoic lesion (yellow arrows).

Figure 20: The hypoechoic lesion (yellow arrows) displays no increased central or peripheral vascularization in **color** duplex sonography.

Figure 21: The hypoechoic lesion (yellow arrows) displays an increased peripheral vascularization in **MV-Flow™**.

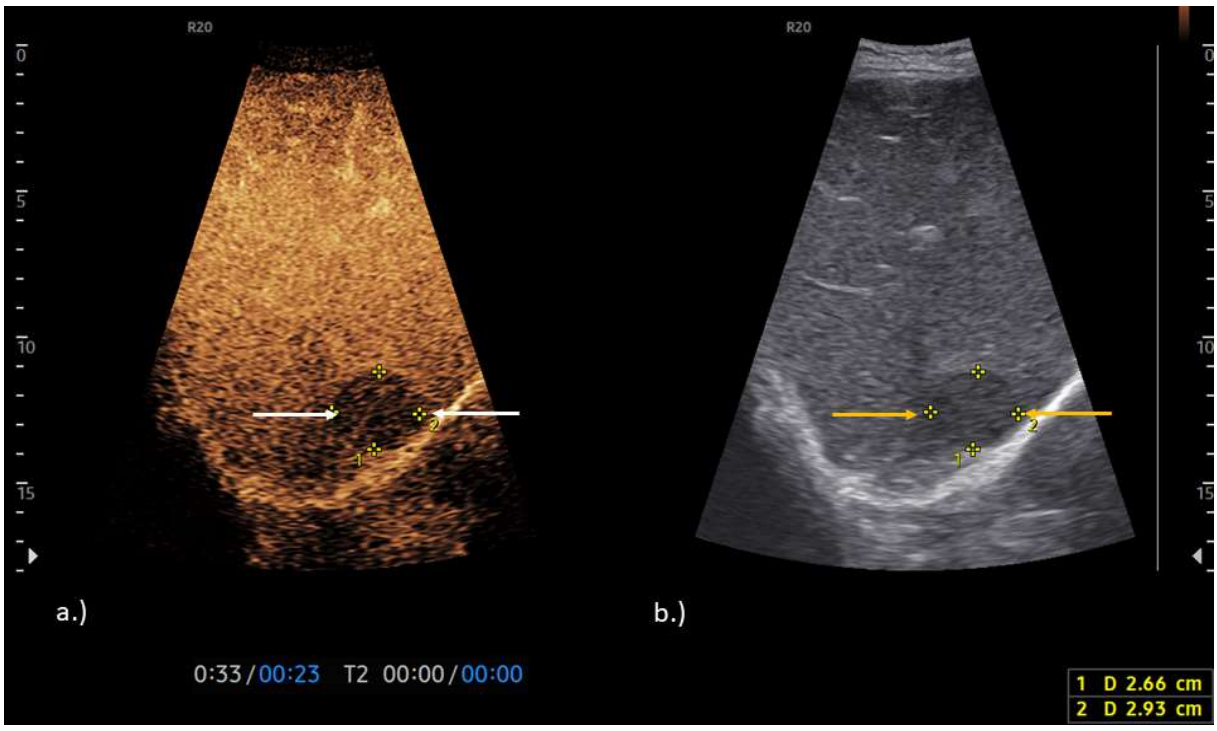

Figure 22: Dual-mode technique showing **CEUS** information (a.) and the B-scan (b.). In the **arterial phase**, the lesion is delineated by moderated enhancement (white arrows). In the B-scan setting the lesion (yellow arrows) it is clearly visible.

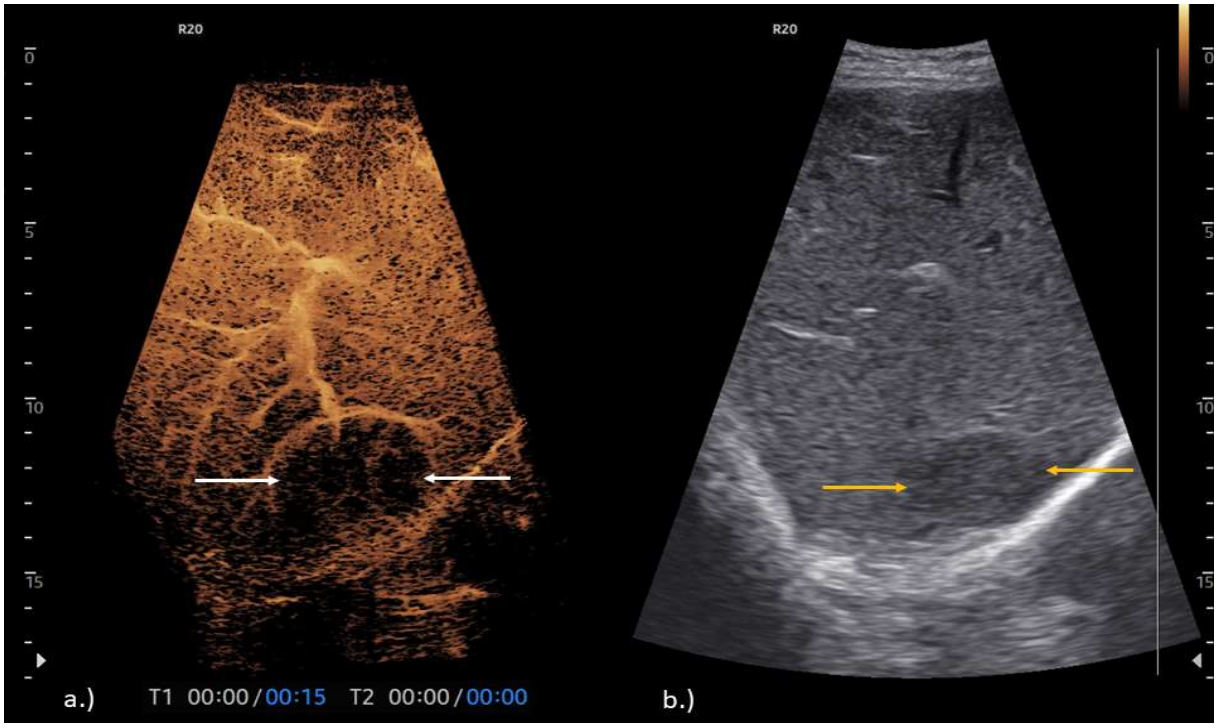

Figure 23: Dual-mode technique showing **MV-CEUS™** (a.) and the B-scan (b.). In the **arterial phase**, the lesion is delineated by poor enhancement (white arrows). In the B-scan setting the lesion (yellow arrows) it is clearly visible. The final diagnosis was a diffuse large B-cell lymphoma.

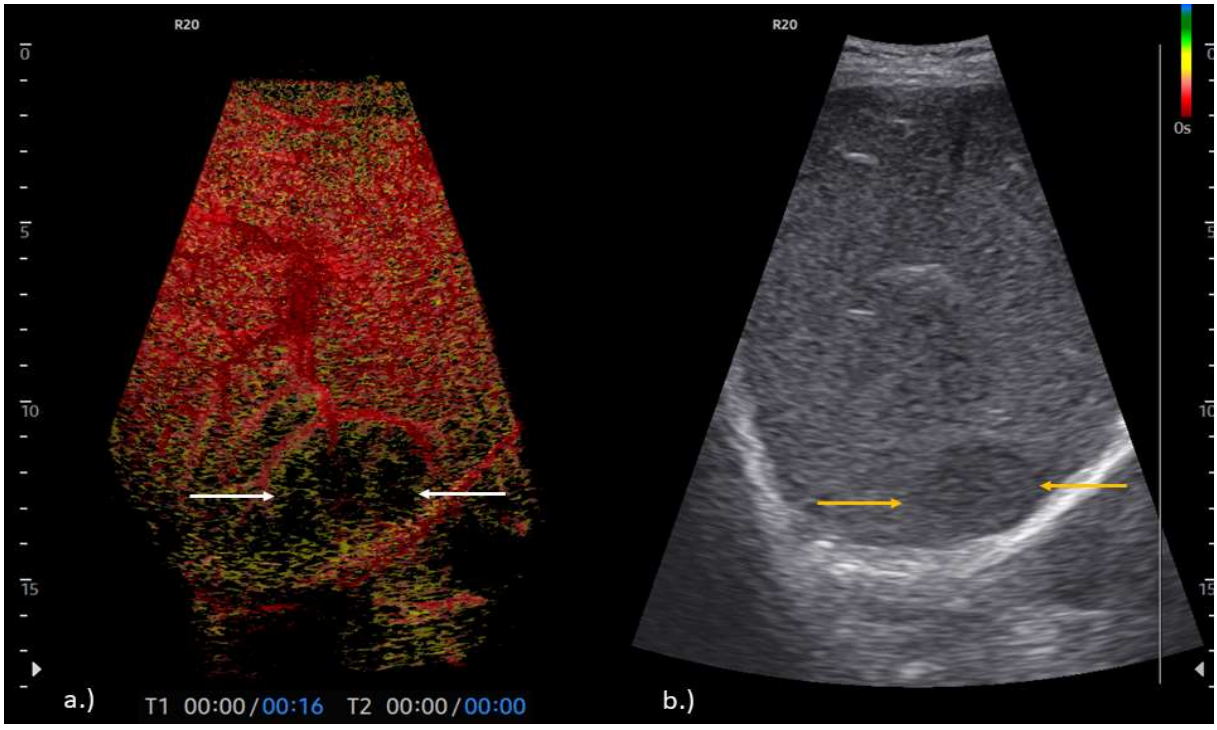

Figure 24: Dual-mode technique showing **Time of arrival** (a.) and the B-scan (b.). In the **arterial phase**, the lesion is delineated by poor enhancement (white arrows). In the B-scan setting the lesion (yellow arrows) it is clearly visible. The final diagnosis was a diffuse large B-cell lymphoma.

Hepatocellular carcinoma (HCC) (Fig. 25-33)

HCC is often diagnosed in cirrhotic livers where conventional imaging may be limited by nodularity and heterogeneity. Compared to standard CEUS, MV-CEUS™ allows for more detailed highlighting of feeding vessels and intranodular microvascular networks. This suggest MV-CEUS™ has a potential role in supporting LI-RADS categorization and providing additional confidence in treatment response assessment [18].

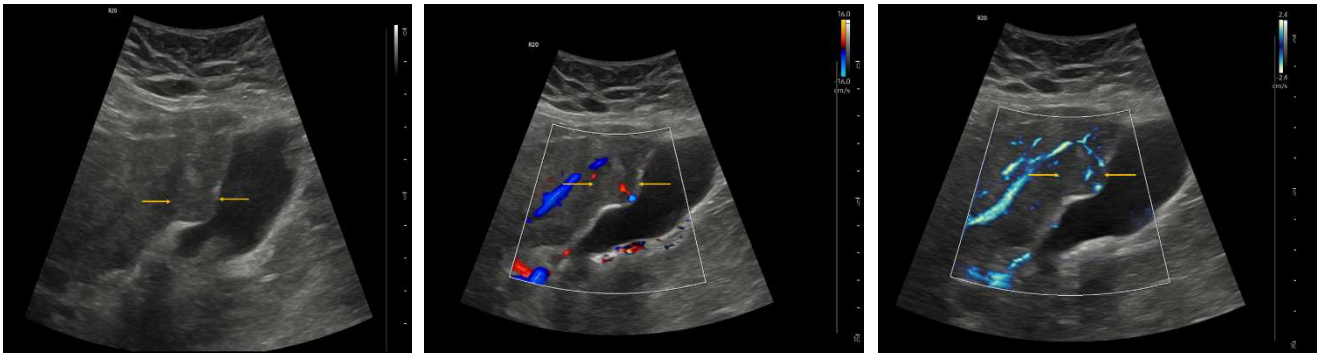

Figure 25: 76-year-old male patient with a nearly isoechoic lesion (yellow arrows) of unknown origin in a cirrhotic liver next to the gallbladder.

Figure 26: The isoechoic lesion (yellow arrows) displays any increase in vascularization in **color** duplex sonography.

Figure 27: The isoechoic lesion (yellow arrows) displays any increase vascularization in **MV-Flow™**.

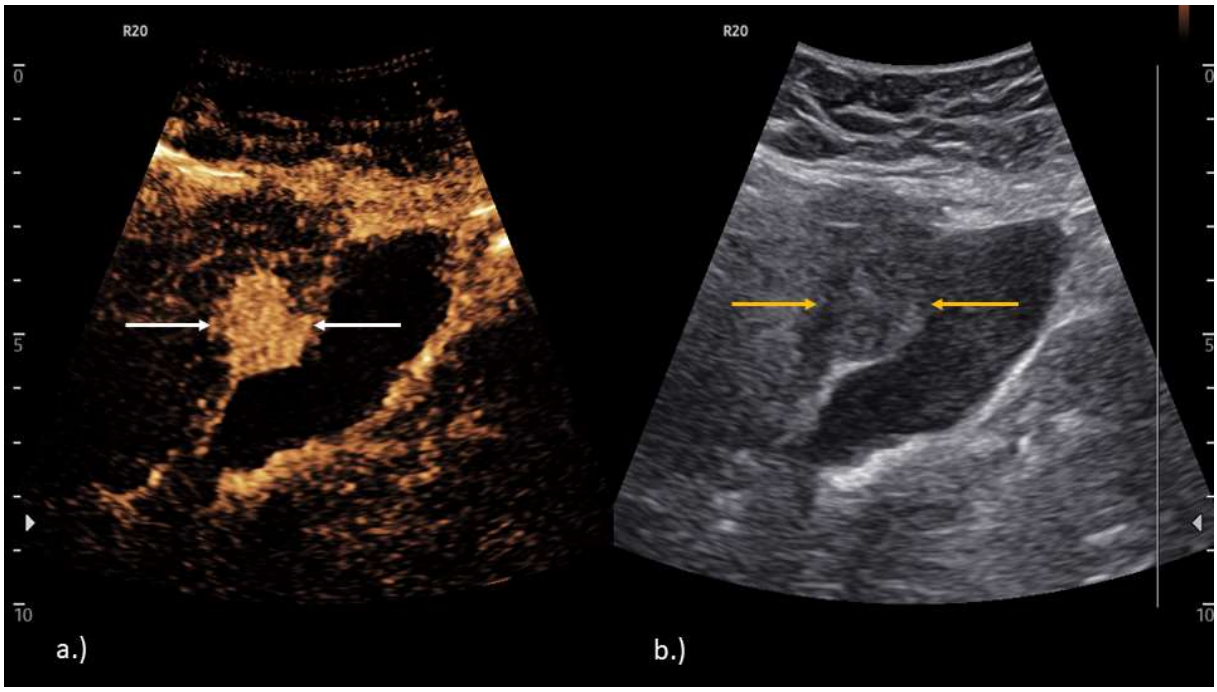

Figure 28: Dual-mode technique showing **CEUS** information (a.) and the B-scan (b.). In the **arterial phase**, the lesion is delineated by intense enhancement (white arrows). In the B-scan setting the lesion (yellow arrows) it is not clearly visible as an isoechoic liver lesion.

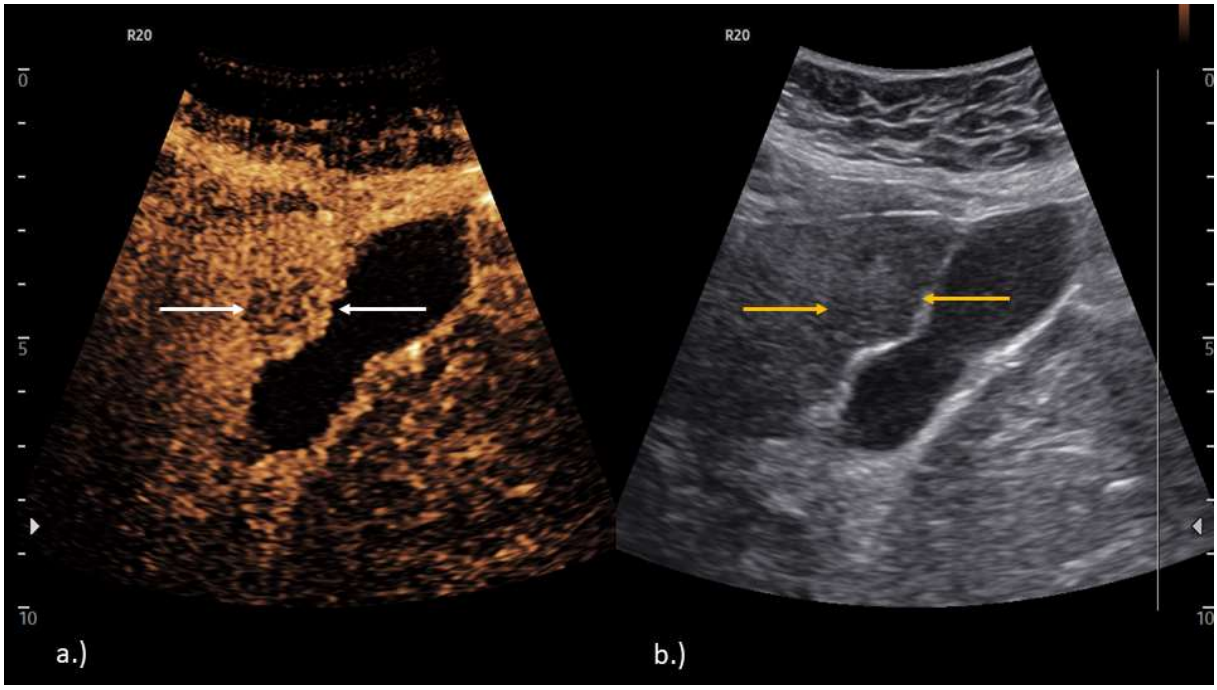

Figure 29: Dual-mode technique showing **CEUS** information (a.) and the B-scan (b.). In the **late phase** after 3 minutes, the lesion (white arrows) becomes visible against the surrounding liver tissue following wash-out. In the B-scan setting the lesion (yellow arrows) it is not clearly visible as an isoechoic liver lesion.

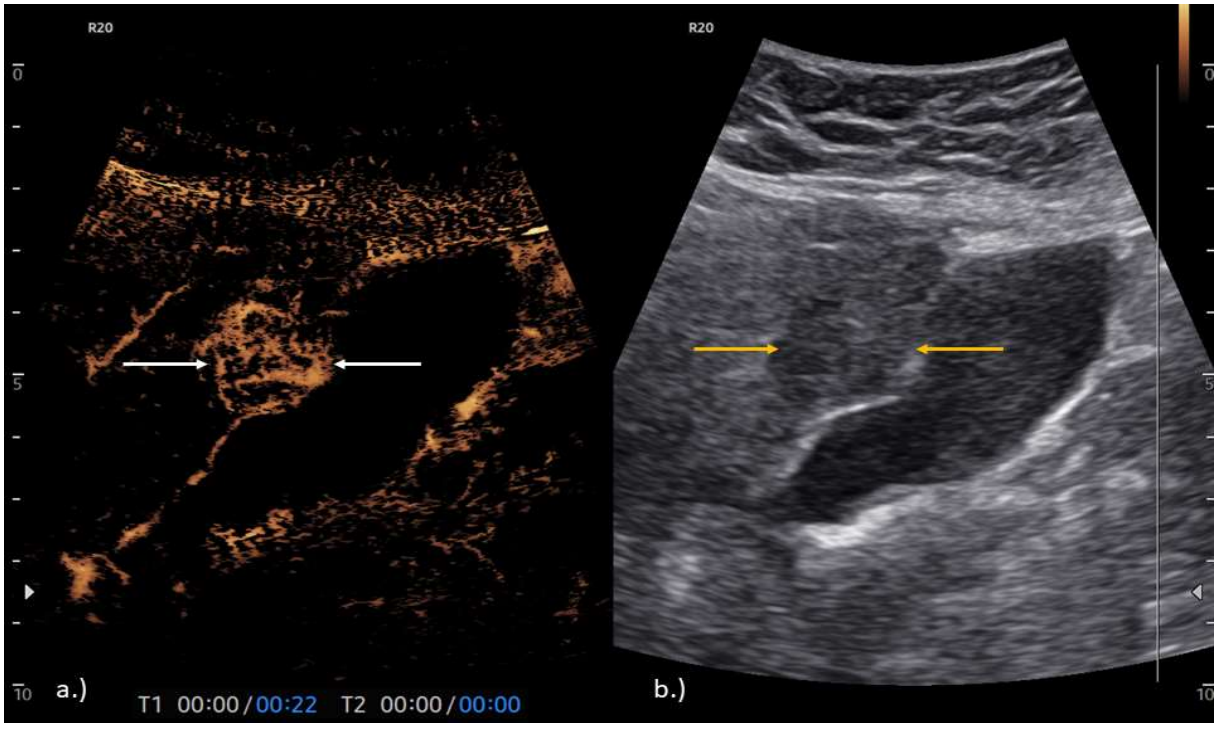

Figure 30: Dual-mode technique showing **MV-CEUS™** (a.) and the B-scan (b.). In the **arterial phase**, the lesion is delineated by intense enhancement (white arrows) in the **MV-CEUS™**, tiny chaotic vessels are visible in the lesion. In the B-scan setting the lesion (yellow arrows) is not clearly visible as an isoechoic liver lesion.

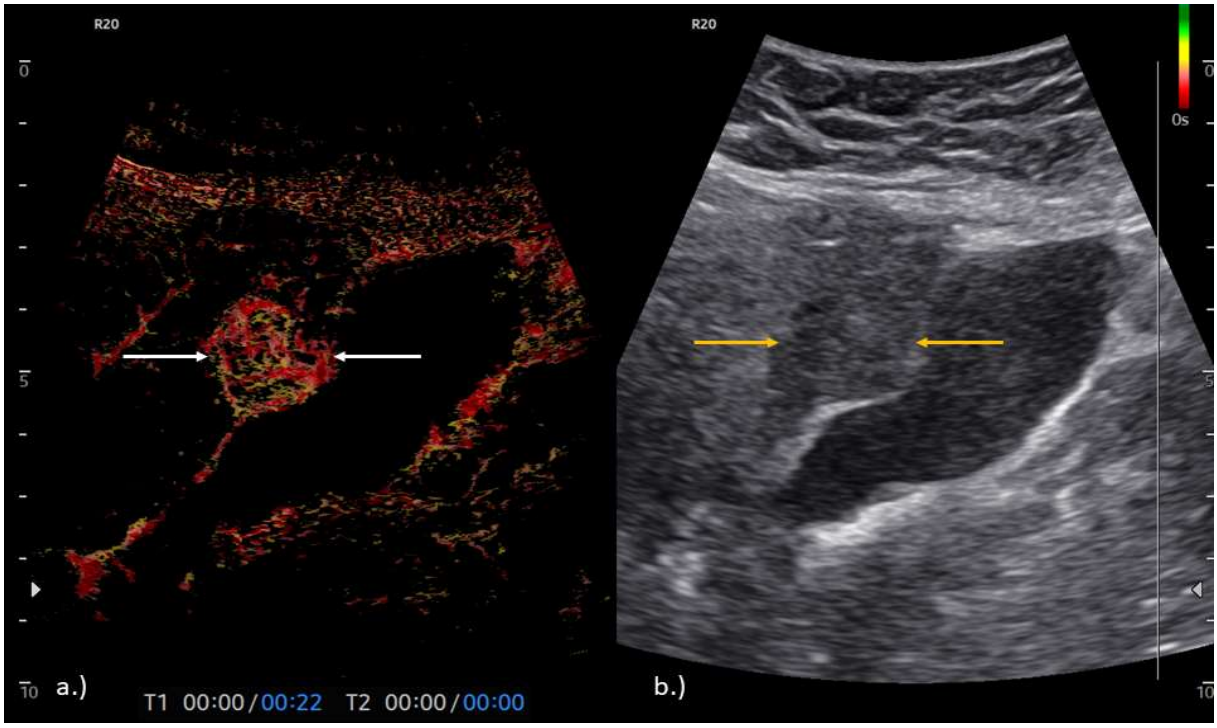

Figure 31: Dual-mode technique showing **Time of arrival** (a.) and the B-scan (b.). In the **arterial phase**, the lesion is delineated by intense enhancement (white arrows), the tiny chaotic vessels show a fast uptake of the contrast agent. In the B-scan setting the lesion (yellow arrows) is not clearly visible as an isoechoic liver lesion.

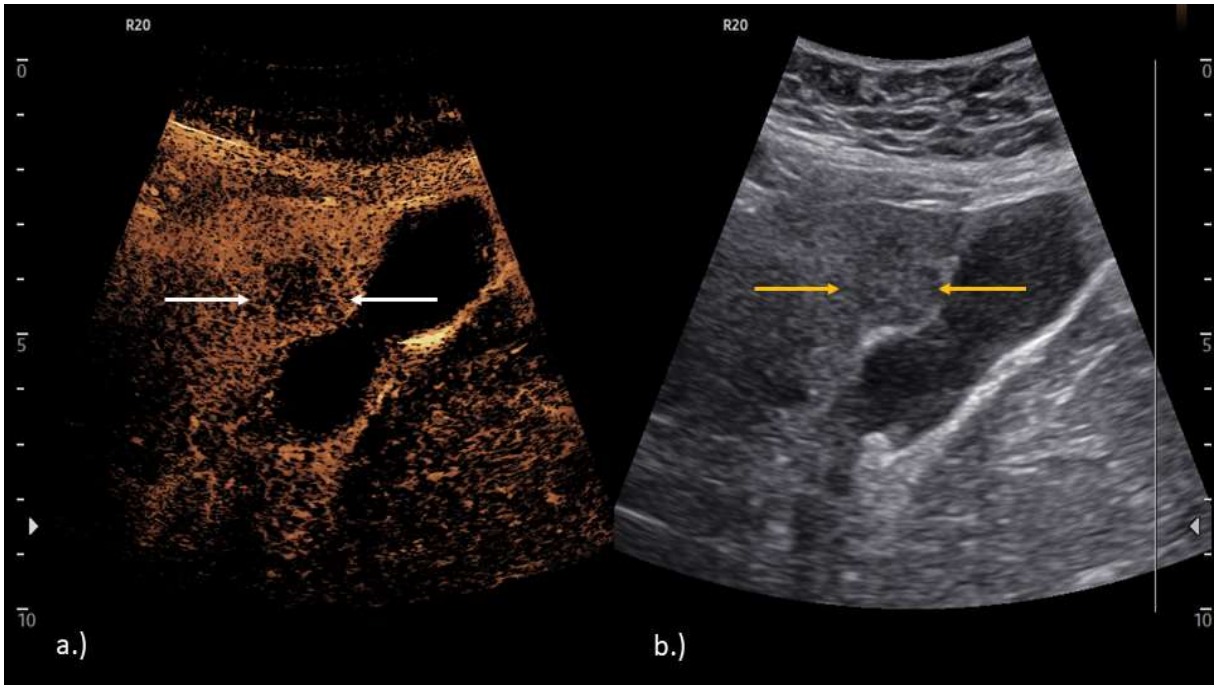

Figure 32: Dual-mode technique showing **MV-CEUS™** (a.) and the B-scan (b.). In the **late phase** close to five minutes, the lesion (white arrows) becomes visible against the surrounding liver tissue following wash-out. In the B-scan setting the lesion (yellow arrows) is not clearly visible as an isoechoic liver lesion. The final diagnosis was a HCC which was confirmed after biopsy.

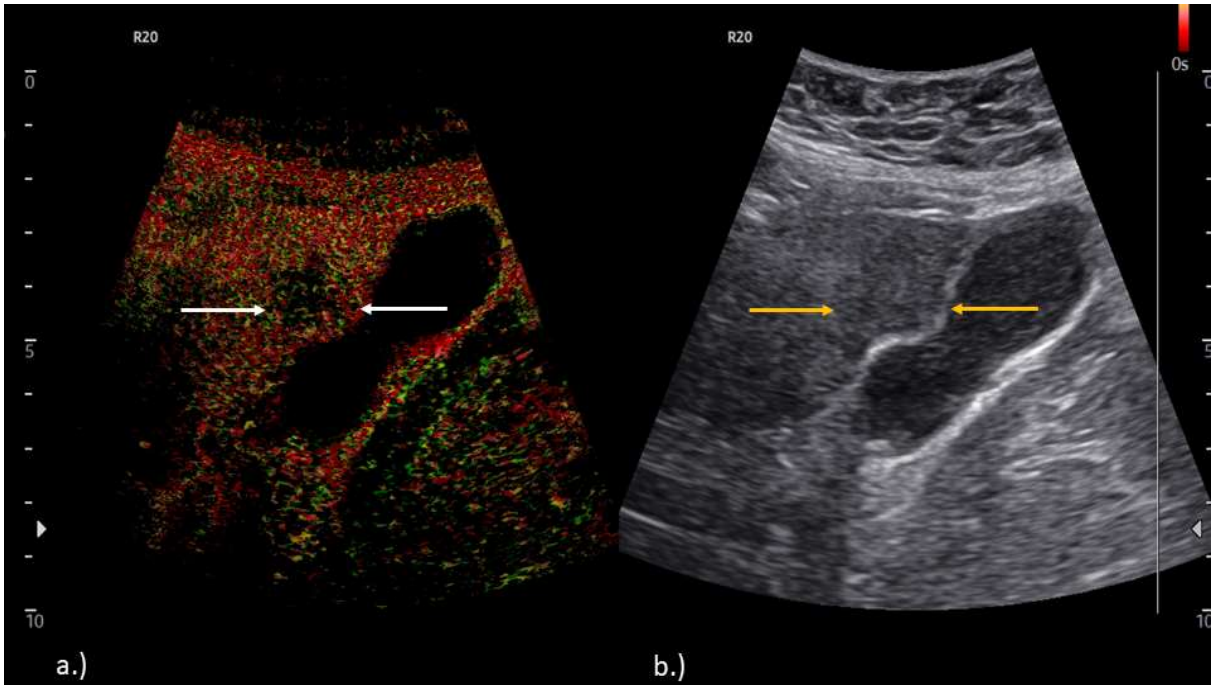

Figure 33: Dual-mode technique showing **Time of arrival** (a.) and the B-scan (b.). In the **late phase** close to five minutes, the lesion (white arrows) becomes visible against the surrounding liver tissue, the **Time of arrival** mode detected the wash out. In the B-scan setting the lesion (yellow arrows) is not clearly visible as an isoechoic liver lesion. The final diagnosis was a HCC which was confirmed after biopsy.

Validating the clinical potential of MV-CEUS™ is crucial next step

Additional investigation is required to establish its clinical role in chronic liver disease, cirrhosis, and interventional guidance.

Chronic liver disease and cirrhosis: Monitoring progression from fibrosis to cirrhosis requires sensitive detection of perfusion changes. MV-CEUS™ can noninvasively assess sinusoidal microcirculation and intrahepatic shunts. These insights may become valuable for staging and for monitoring antifibrotic therapies.

Interventional guidance: Ultrasound is frequently used during ablative procedures or biopsies. Real-time MV-CEUS™ could help identify vital tumor remnants after ablation and guide targeted sampling of suspicious microvascular "hot spots."

Other Organs (Fig. 34-39)

Limitation: In accordance with the EFSUMB guidelines and recommendations for the clinical practice of CEUS in non-hepatic applications [33], contrast-enhanced ultrasound is used off-label in renal assessment. However, they recommend several indications for the use of CEUS in the kidney.

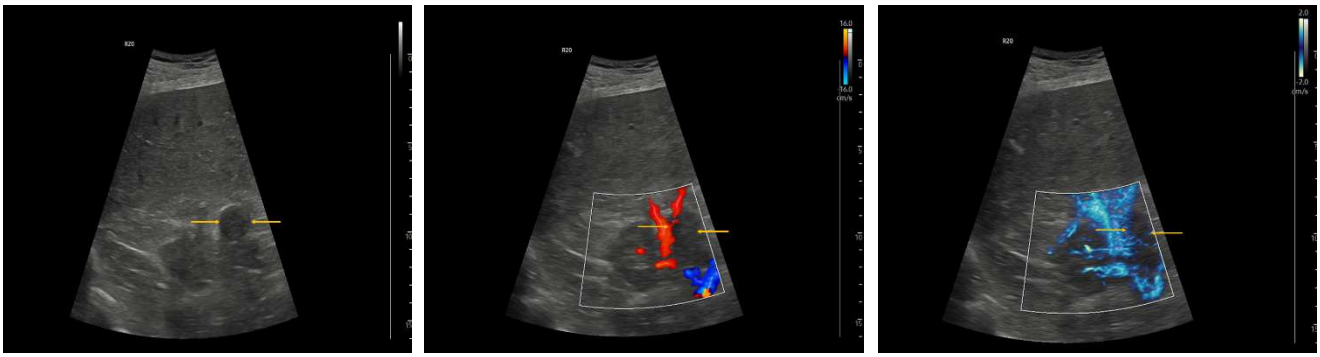

Figure 34: 67-year-old female patient with a nearly hypoechoic lesion (yellow arrows), in the baseline CT examination a hemorrhage cyst of the right kidney was described.

Figure 35: The hypoechoic lesion (yellow arrows) displays no vascularization in **color** duplex sonography.

Figure 36: The hypoechoic lesion (yellow arrows) displays no vascularization in **MV-Flow™**.

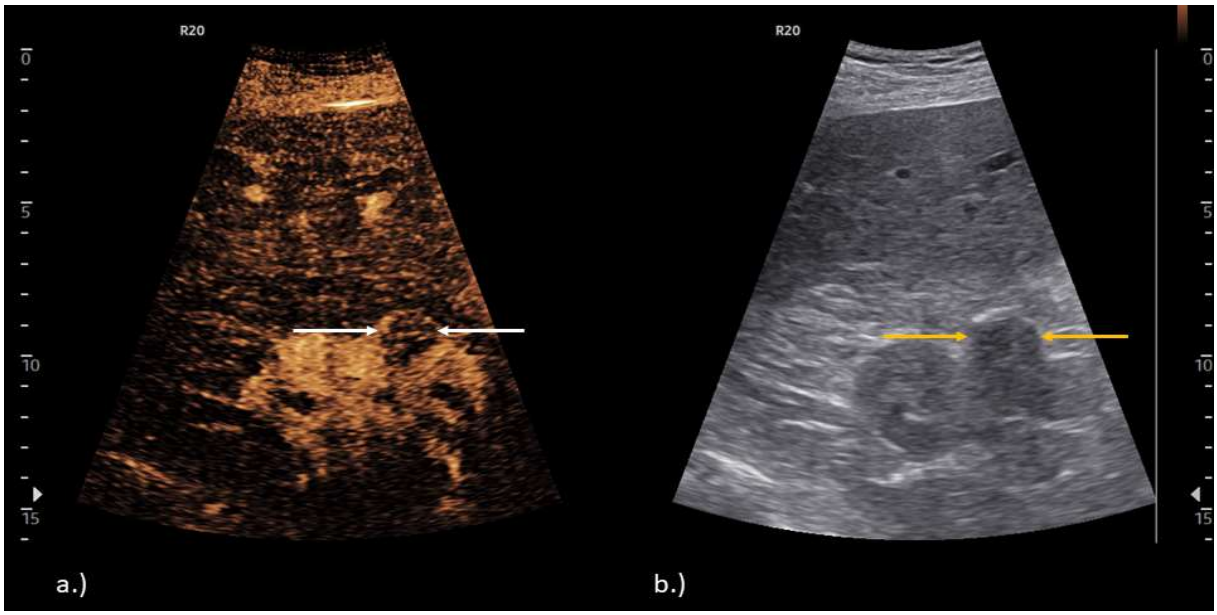

Figure 37: Dual-mode technique showing **CEUS** information (a.) and the B-scan (b.). In the **arterial phase**, the lesion is delineated by poor enhancement (white arrows). In the B-scan setting the lesion (yellow arrows) is clearly visible as a hypoechoic kidney lesion.

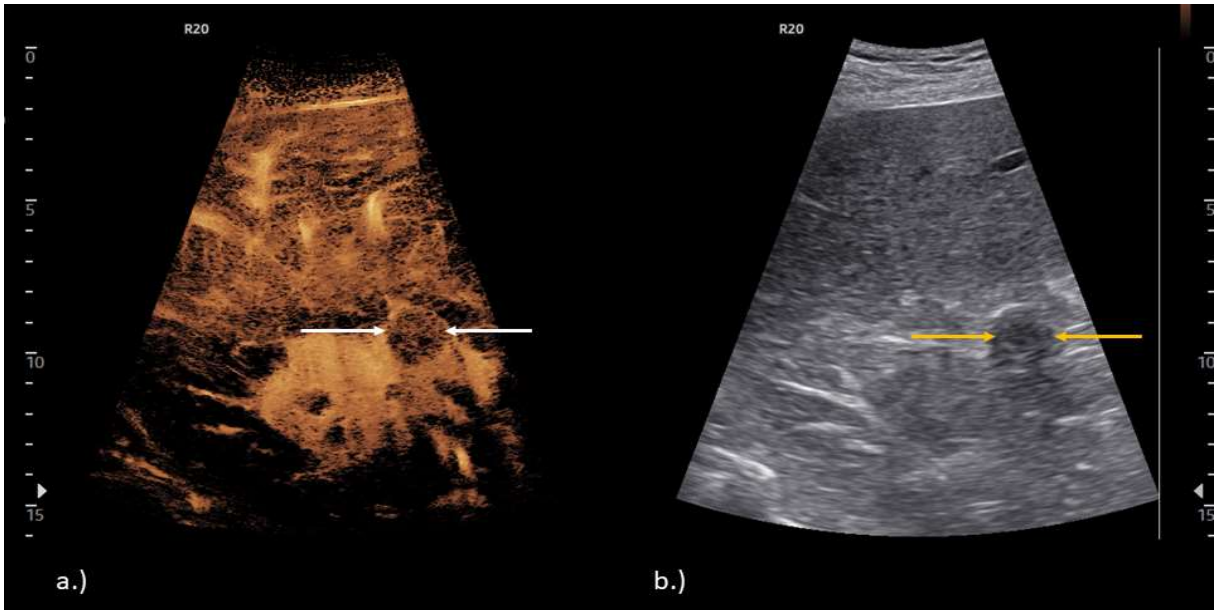

Figure 38: Dual-mode technique showing **MV-CEUS™** (a.) and the B-scan (b.). In the **arterial phase**, the lesion is delineated by poor enhancement (white arrows) in the **MV-CEUS™** tiny vessels are visible in the lesion. In the B-scan setting the lesion (yellow arrows) is clearly visible as a hypoechoic kidney lesion. The final diagnosis was a papillary renal cell cancer which was confirmed after surgery.

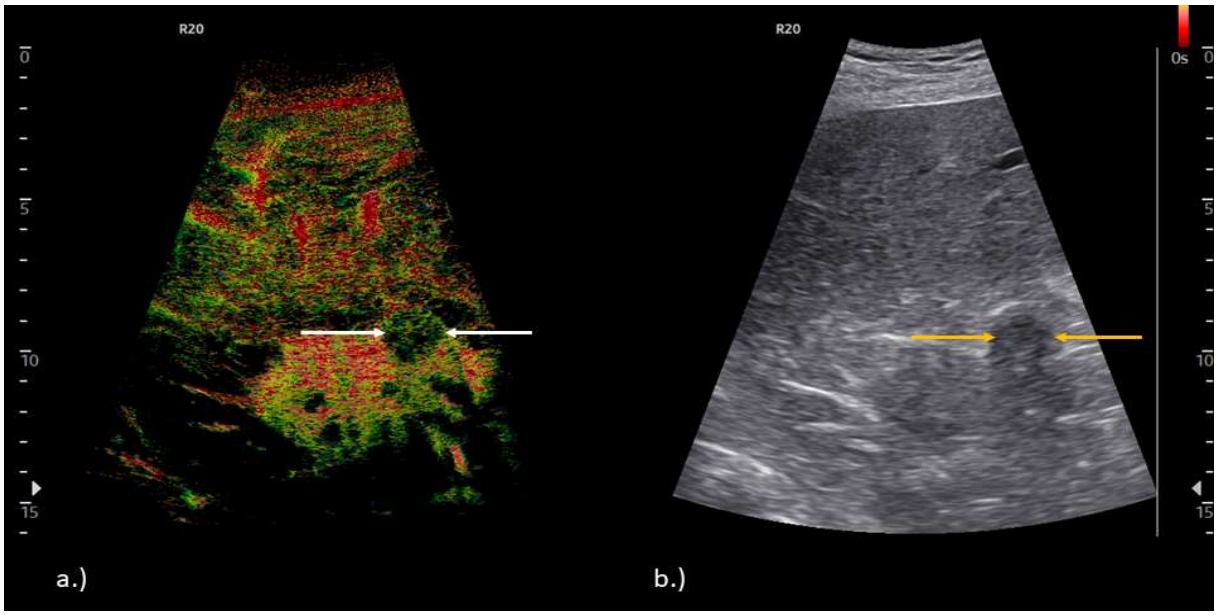

Figure 39: Dual-mode technique showing **Time of arrival** (a.) and the B-scan (b.). In the **arterial phase**, the lesion is delineated by poor enhancement (white arrows), the tiny vessels show a very slow uptake of the contrast agent. In the B-scan setting the lesion (yellow arrows) is clearly visible as a hypoechoic kidney lesion. The final diagnosis was a papillary renal cell cancer which was confirmed after surgery.

Discussion

While ultrasound is a widely used, safe, and cost-effective imaging modality, its resolution limitations have historically been a major drawback. The spatial resolution of conventional ultrasound ranges between 0.4 and 2 mm, depending on probe frequency [13]. This is sufficient for macrovessels but not for capillary-level architecture, which is essential for oncologic imaging [19].

CEUS partly addresses this gap by detecting blood flow at the capillary level, but the microvascular structure remains unresolved. Super Resolution Imaging directly addresses this limitation by providing subwavelength vascular reconstruction. [20-24].

A well-known challenge is the dependency of SR imaging on microbubble concentration. Low concentrations prolong acquisition times, while high concentrations, as typically used in routine CEUS, complicate bubble localization [25-26]. New algorithms and hardware improvements are therefore crucial to bring SR imaging from academic research into everyday practice [27].

Compared with CT and MRI, ultrasound (including CEUS and SR imaging) offers several distinct advantages:

- Safety: no ionizing radiation, no nephrotoxic contrast agents.
- Real-time imaging: allows immediate clinical decisions and interventional guidance.
- Repeatability: can be performed frequently, enabling close therapy monitoring.
- Cost-effectiveness: ultrasound systems are widely available, lowering healthcare costs.

However, CT and MRI still surpass ultrasound in whole-organ staging, detection of extrahepatic disease, and reproducibility across centers. For this reason, SR imaging should be viewed as a complementary tool rather than a replacement. It will likely be integrated into multimodal imaging pathways, where it provides unique microvascular information that CT and MRI cannot match.

Future Perspectives

Following the EFSUMB guidelines [33], the potential of SR imaging extends beyond the liver. Applications in renal tumors, pancreatic lesions, and musculoskeletal microcirculation are being explored, although contrast agents are off-label for these applications. In oncology, the technique may serve as a biomarker for treatment response, particularly in immunotherapy where microvascular normalization is a surrogate of efficacy.

Integration with artificial intelligence (AI) could further enhance clinical usability by automating bubble tracking, motion correction, and feature extraction. AI-driven quantitative indices may standardize SR imaging assessments and facilitate large multicenter studies.

Another exciting perspective is the combination of SR imaging with therapeutic ultrasound (e.g. high-intensity focused ultrasound, HIFU). Here, imaging and therapy could be merged into theranostics approaches, enabling treatment monitoring at the microvascular level in real time.

Finally, the ongoing miniaturization of ultrasound systems promises to make advanced imaging accessible at the bedside, in intensive care, and in low-resource settings. This democratization of technology could significantly improve global liver cancer care.

Conclusion

Ultrasound remains the backbone of liver imaging because it is safe, versatile, and cost-effective. CEUS has transformed lesion characterization by enabling real-time assessment of perfusion dynamics. The advent of Super Resolution Imaging now marks the next step, offering capillary-level detail that was previously unattainable in clinical practice. Due to the new availability of the Super Resolution Imaging technology, knowledge transfer to other organs (Fig. 34-39) will be expected and the first scientific papers are already published [28-32].

By enabling precise visualization of microvascular networks, SR imaging has the potential to refine differential diagnosis, improve treatment response monitoring, and guide targeted interventions. Its integration into routine practice, alongside CT and MRI, could significantly enhance the diagnostic armamentarium for liver diseases. In our experience the Super Resolution Imaging technique also offers significant advantages in the evaluation of unclear hemorrhage cystic renal lesions, as described in the EFSUMB guidelines [33].

Future research should focus on validating these techniques in large patient cohorts, standardizing protocols, and exploring applications in other abdominal and extra-abdominal organs. If these challenges are addressed, Super Resolution Imaging may expand the role of ultrasound in oncology and hepatology, establishing it not only as a screening tool but as a key imaging modality for precision medicine.

Reference

[1] Ferraioli, G., et al., 2018. Ultrasound in liver disease. World Journal of Gastroenterology.

[2] Piorkowska, K., et al., 2018. Safety of ultrasound in pregnancy and pediatrics. Journal of Ultrasound in Medicine.

[3] Sidhu PS, Clevert DA, Deganello A, Piskunowicz M, Cantisani V, Fischer T; European Society of Radiology (ESR). Controversies in contrast-enhanced ultrasound (CEUS): pregnancy, paediatric, abdominal trauma, complex renal cysts, and endovascular aortic repair follow-up. Insights Imaging. 2025 Aug 15;16(1):179.

[4] Geyer T, Rübenthaler J, Froelich MF, Sabel L, Marschner C, Schwarze V, Clevert DA. Contrast-Enhanced Ultrasound for Assessing Abdominal Conditions in Pregnancy. Medicina (Kaunas). 2020 Dec 8;56(12):675

[5] Schwarze V, Froelich MF, Marschner C, Knösel T, Rübenthaler J, Clevert DA. Safe and pivotal approaches using contrast-enhanced ultrasound for the diagnostic workup of non-obstetric conditions during pregnancy, a single-center experience. Arch Gynecol Obstet. 2021 Jan;303(1):103-112

[6] Schwarze V, Marschner C, Negrão de Figueiredo G, Rübenthaler J, Clevert DA. Single-Center Study: Evaluating the Diagnostic Performance and Safety of Contrast-Enhanced Ultrasound (CEUS) in Pregnant Women to Assess Hepatic Lesions. Ultraschall Med. 2020 Feb;41(1):29-35.

[7] Runtemund, J., et al., 2022. Economic aspects of ultrasound compared to CT and MRI in liver imaging. European Radiology.

[8] Dietrich, C.F., et al., 2019. Contrast-enhanced ultrasound (CEUS) for the characterization of focal liver lesions. Ultraschall in der Medizin.

[9] Wu J, Xu W, Li L, Xie W, Tang B. Real-Time Super-Resolution Ultrasound Imaging for Monitoring Tumor Response During Intensive Care Management of Oncologic Emergencies. Cancer Biother Radiopharm. 2025 Sep 4. doi: 10.1177/10849785251376112.

[10] Zeng QQ, An SZ, Chen CN, Wang Z, Liu JC, Wan MX, Zong YJ, Jian XH, Yu J, Liang P. Focal liver lesions: multiparametric microvasculature characterization via super-resolution ultrasound imaging. Eur Radiol Exp. 2024 Dec 5;8(1):138.

[11] He J, Yi H, Tang D, Zhang X, Cui X, Zhang W. Differentiating benign and malignant superficial lymph nodes using super-resolution contrast enhanced ultrasound - a pilot study. BMC Med Imaging. 2025 May 19;25(1):170.

[12] Apfelbeck M, Loupas T, Chaloupka M, Clevert DA. Improved diagnostic confidence using Super Resolution CEUS imaging in testicular lesions. Clin Hemorheol Microcirc. 2024;88(s1):S113-S125.

[13] O M Viessmann 1, R J Eckersley, K Christensen-Jeffries, M X Tang, C Dunsby Acoustic super-resolution with ultrasound and microbubbles Phys Med Biol. 2013 Sep 21;58(18):6447-58

[14] M. Siepmann, G. Schmitz, J. Bzyl, M. Palmowski, and F. Kiessling, "Imaging tumor vascularity by tracing single microbubbles," in Proc. IEEE Int. Ultrason. Symp., Oct. 2011, pp. 1906–1909.

[15] D. Ackermann and G. Schmitz, "Detection and tracking of multiple microbubbles in ultrasound B-Mode images," IEEE Trans. Ultrason., Ferroelectr., Freq. Control, vol. 63, no. 1, pp. 72–82, Jan. 2016.

[16] K. Christensen-Jeffries, R. J. Browning, M.-X. Tang, C. Dunsby, and R. J. Eckersley, "In vivo acoustic super-resolution and super-resolved velocity mapping using microbubbles," IEEE Trans. Med. Imag., vol. 34, no. 2, pp. 433–440, Feb. 2015.

[17] C. Errico et al., "Ultrafast ultrasound localization microscopy for deep super-resolution vascular imaging," Nature, vol. 527, no. 7579, pp. 499–502, Nov. 2015.

[18] Siu Xiao T, Kuon Yeng Escalante CM, Tahmasebi A, Kono Y, Piscaglia F, Wilson SR, Medellin-Kowalewski A, Rodgers SK, Planz V, Kamaya A, Fetzer DT, Berzigotti A, Radu IP, Sidhu PS, Wessner CE, Bradigan K, Eisenbrey JR, Forsberg F, Lyshchik A. Combining CEUS and CT/MRI LI-RADS major imaging features: diagnostic accuracy for classification of indeterminate liver observations in patients at risk for HCC. Abdom Radiol (NY). 2025 May;50(5):2066-2077.

[19] Tang M X, Mulvana H, Gauthier T, Lim A K P, Cosgrove D O, Eckersley R J and Stride E 2011 Quantitative contrast-enhanced ultrasound imaging: a review of sources of variability Interface Focus 1 520–39

[20] O. Couture, B. Besson, G. Montaldo, M. Fink, and M. Tanter, Microbubble ultrasound super localization imaging (MUSLI), IEEE Int. Ultrason. Symp., Oct. 2011, pp. 1285–1287.

[21] M. Siepmann, G. Schmitz, J. Bzyl, M. Palmowski, and F. Kiessling, "Imaging tumor vascularity by tracing single microbubbles," in Proc. IEEE Int. Ultrason. Symp., Oct. 2011, pp. 1906–1909.

[22] D. Ackermann and G. Schmitz, "Detection and tracking of multiple microbubbles in ultrasound B-Mode images," IEEE Trans. Ultrason., Ferroelectr., Freq. Control, vol. 63, no. 1, pp. 72–82, Jan. 2016.

[23] K. Christensen-Jeffries, R. J. Browning, M.-X. Tang, C. Dunsby, and R. J. Eckersley, "In vivo acoustic super-resolution and super-resolved velocity mapping using microbubbles," IEEE Trans. Med. Imag., vol. 34, no. 2, pp. 433–440, Feb. 2015.

[24] C. Errico et al., “Ultrafast ultrasound localization microscopy for deep super-resolution vascular imaging,” Nature, vol. 527, no. 7579, pp. 499–502, Nov. 2015.

[25] Couture, O.; Hingot, V.; Heiles, B.; Muleki-Seya, P.; Tanter, M. Ultrasound Localization Microscopy and Super-Resolution: A State of the Art. IEEE Trans. Ultrason. Ferroelectr. Freq. Control 2018, 65, 1304–1320.

[26] Brown, J.; Christensen-Jeffries, K.; Harput, S.; Zhang, G.; Zhu, J.; Dunsby, C.; Tang, M.X.; Eckersley, R.J. Investigation of Microbubble Detection Methods for Super-Resolution Imaging of Microvasculature. IEEE Trans. Ultrason. Ferroelectr. Freq. Control 2019, 66, 676–691

[27] Qiyang Chen, Hyeju Song, Jaesok Yu, Kang Kim Current Development and Applications of Super-Resolution Ultrasound Imaging Sensors (Basel) . 2021 Apr 1;21(7):2417.

[28] Yang L, Li X, Wang Z, Li Q, Fu J, Zou X, Liang X, Liu X, Zhang R, Chen J, Xie H, Huang Y, Zhou J. Super-Resolution Ultrasound Radiomics Can Predict the Upstaging of Ductal Carcinoma In Situ. Cancer Med. 2025 Aug;14(15):e71155.

[29] Huang X, Zhang Y, Hu Y, Pan J, Huang X, Zhang J, Pu H, Chen Y, Deng Q, Zhou Q. Combining Super-Resolution Imaging and Shear Wave Elastography for Enhanced Risk Assessment of Moderate-to-Severe Renal Fibrosis in Chronic Kidney Disease Patients. Int J Nephrol Renovasc Dis. 2025 Jun 30;18:187-199.

[30] Amin Naji M, Panduro NS, Tabatabaei Majd SMM, Hansen LN, Taghavi I, Gundlach C, T McDermott A, omov BG, Nielsen MB, Sørensen CM, Jensen JA. Human lymph node microvascular imaging using a fast contrast-free super-resolution ultrasound technique.Sci Rep. 2025 Jul 2;15(1):23061. doi: 10.1038/s41598-025-08483-4.

[31] Gao JY, Hou C. Progresses and clinical application of super-resolution ultrasound imaging: a narrative review. Ultrasound J. 2025 Jun 16;17(1):29.

[32] Butler MB, Papageorgiou G, Kanoulas ED, Voulgaridou V, Wijkstra H, Mischi M, Mannaerts CK, McDougall S, Duncan WC, Lu W, Sboros V. Mapping of prostate cancer microvascular patterns using super-resolution ultrasound imaging. Eur Radiol Exp. 2025 Feb 20;9(1):25.

[33] Sidhu PS, Cantisani V, Dietrich CF, Gilja OH, Saftoiu A, Bartels E, Bertolotto M, Calliada F, Clevert DA, Cosgrove D, Deganello A, D'Onofrio M, Drudi FM, Freeman S, Harvey C, Jenssen C, Jung EM, Klauser AS, Lassau N, Meloni MF, Leen E, Nicolau C, Nolsoe C, Piscaglia F, Prada F, Prosch H, Radzina M, Savelli L, Weskott HP, Wijkstra H. The EFSUMB Guidelines and Recommendations for the Clinical Practice of Contrast-Enhanced Ultrasound (CEUS) in Non-Hepatic Applications: Update 2017 (Long Version). Ultraschall Med. 2018 Apr;39(2):e2-e44.

Disclaimer

* The features mentioned in this document may not be commercially available in all countries and may contain more detailed information than officially approved. Due to regulatory reasons, their future availability cannot be guaranteed.
* Do not distribute this document to customers unless relevant regulatory and legal affairs officers approve such distribution.
* Images may have been cropped to better visualize their pathology.
* This study was funded by Samsung Medison to aid customers in their understanding.
* The results reflect the experience of a single user at a single site, and may not be representative of results that may be obtained in other settings. Healthcare professionals should rely on their own professional judgment and experience when interpreting these results and making clinical decision.

Scan code or Visit
Samsunghealthcare.com
to learn more

SAMSUNG MEDISON CO., LTD.
© 2025 Samsung Medison All Rights Reserved.

Samsung Medison reserves the right to modify any design, packaging,
Specifications and features shown herein, without prior notice or obligation.